

Thus AIDS-KS cells synthesize and release relatively large amounts of biologically active bFGF-like molecules and IL-1 that can induce self-proliferation. In addition to this autocrine growth effect, the released bFGF-like molecules also induce proliferation of normal endothelial cells (paracrine). In the human KS lesion, the proliferation of spindle cells, endothelial cells, and fibroblasts is associated with angiogenesis and inflammatory cell infiltration (2-6). Interaction among endothelial cells, fibroblasts, and cells of the immune system induced by the bFGF-like molecule and IL-1 (and possibly by the other cytokines expressed by AIDS-KS cells) could be responsible for the lesion induced in the nude mouse by the AIDS-KS cells (6). The data presented here thus support the idea (5, 6) that, in humans, the putative novel growth factor released by CD4<sup>+</sup> T cells infected with one of the human retroviruses (5) initiates cellular events that lead to the production of cytokines and consequent cell growth and histologic changes relevant to the pathogenesis of AIDS-associated KS.

- bovine cells may reflect heterogeneity of bFGF-related mRNA in different cells derived from different species, or may be due to the presence of precursor transcripts (such as the 6.8- to 7-kb band) containing untranslated flanking regions, or to the use of different initiation or termination sites of transcription (9-11).
13. P. Delli Bovi *et al.*, *Cell* **50**, 729 (1987).
  14. M. Terada *et al.*, *Proc. Natl. Acad. Sci., U.S.A.* **84**, 2980 (1987).
  15. The *hst* probe was provided by M. Terada [see (14)].
  16. T. Maciag, paper presented at Congress on Cytokines and Growth Factors, Philadelphia, PA, 25 to 28 October 1987.
  17. C. J. March *et al.*, *Nature* **315**, 641 (1985).
  18. S. Clark and R. Kamen, *Science* **236**, 1229 (1987); J. Y. Chan, D. J. Slamon, S. D. Nimer, D. W. Golde, J. C. Gasson, *Proc. Natl. Acad. Sci. U.S.A.* **83**, 8669 (1986).
  19. G. G. Wong *et al.*, *Science* **228**, 810 (1985).
  20. S. Nakamura, unpublished data.
  21. J. Massague, *Cell* **49**, 437 (1987); K. Takehara, E. C. Leroy, G. R. Grotendorst, *ibid.*, p. 415; M. B. Sporn *et al.*, *Proc. Natl. Acad. Sci. U.S.A.* **83**, 4167 (1986); R. Derynck *et al.*, *Cancer Res.* **47**, 707 (1987); T. A. Mustoe *et al.*, *Science* **237**, 1333 (1987).
  22. T. Collins, D. Ginsburg, J. M. Boss, S. H. Orkin, J. S. Pober, *Nature* **316**, 748 (1985).
  23. For the RNA blot analysis the filters were hybridized with TGF- $\alpha$  (48-mer), angiogenin (48-mer), M-CSF (48-mer), TNF- $\alpha$  and - $\beta$  oligonucleotide probes (both 50-mer) derived from their respective human cDNA sequences.
  24. The antiserum to bFGF is a polyclonal rabbit antise-

- rum (R773) to a synthetic peptide (aa [1-24]-NH<sub>2</sub>) of bovine bFGF, and was provided by A. Baird.
25. D. Moscatelli, J. Joseph-Silverstein, R. Mancijas, D. B. Rifkin, *Proc. Natl. Acad. Sci. U.S.A.* **84**, 5778 (1987).
  26. P. E. Auron *et al.*, *J. Immunol.* **138**, 1447 (1987).
  27. The bFGF antibodies, purchased from R&D Systems, are the affinity-purified immunoglobulin G (IgG) fraction of a neutralizing polyclonal rabbit antiserum to affinity-purified native bovine brain bFGF.
  28. T. A. Liberemann *et al.*, *EMBO J.* **6**, 1627 (1987).
  29. The IL-1 antibodies, purchased from Endogen, were the highly purified IgG fraction of a polyclonal rabbit antiserum to human IL-1.
  30. T. Maniatis, E. F. Fritsch, J. Sambrook, *Molecular Cloning: A Laboratory Manual* (Cold Spring Harbor Laboratory, Cold Spring Harbor, NY, 1982).
  31. The probes (bFGF-1: 39-mer, bFGF-2: 42-mer, and bFGF-3: 48-mer) were derived, respectively, from nucleotides 160-198, 342-383, and 421-468 of the published human bFGF cDNA sequences (11) and were end-labeled by incubation with <sup>32</sup>P adenosine triphosphate and T4 polynucleotide kinase.
  32. M. Jaye *et al.*, *Science* **233**, 541 (1986).
  33. J. K. Laemmli, *Nature* **227**, 680 (1970).
  34. We thank M. Raffeld and O. Segatto for discussions and comments, M. Johnston and J. Hofman for technical help, and E. Vinar and C. Lease for manuscript preparation. P.B. was supported by the Swedish Medical Research Council and Cancer Society, EORTC, and the E. Fernstrom Foundation.

3 October 1988; accepted 23 November 1988

#### REFERENCES AND NOTES

1. M. Kaposi, *Arch. Dermatol. Syphil.* **4**, 265 (1972); A. C. Templeton, *Pathol. Ann.* **16**, 315 (1981).
2. G. J. Gottlieb *et al.*, *Am. J. Dermatopathol.* **3**, 111, (1981); B. Safai *et al.*, *Ann. Intern. Med.* **103**, 744 (1985).
3. J. L. Ziegler, A. C. Templeton, C. L. Vogel, *Sem. Oncol.* **11** (no. 1), 47 (1984); R. Russel Jones *et al.*, *J. Clin. Pathol.* **39**, 742 (1986).
4. F. H. Cox and E. B. Helwig, *Cancer* **12**, 289 (1959); A. R. Harwood *et al.*, *Am. J. Med.* **67**, 259 (1979); R. A. Hoshaw and R. A. Schwartz, *Arch. Dermatol.* **116**, 1280 (1980); A. C. Templeton, *Cancer* **30**, 854 (1972); J. Costa and A. S. Rabson, *Lancet* **1**, 58 (1983); J. J. Brooks, *ibid.* **ii**, 1309 (1986).
5. S. Nakamura *et al.*, *Science* **242**, 426 (1988).
6. S. Z. Salahuddin *et al.*, *ibid.*, p. 430.
7. T. Maciag, I. S. Cerundolo, P. R. Kelley, R. Forand, *Proc. Natl. Acad. Sci. U.S.A.*, **76**, 5674 (1979); D. Gospodarowicz, H. Bialecki, G. Greenburg, *J. Biol. Chem.* **253**, 3736 (1978); J. Folkman and M. Klagsbrun, *Science* **235**, 442 (1987); D. Gospodarowicz, G. Neufeld, L. Schweigerer, *Mol. Cell. Endocrinol.* **46**, 187 (1986); R. Montesano, J. D. Vassalli, A. Baird, R. Guillemin, L. Orci, *Proc. Natl. Acad. Sci. U.S.A.* **83**, 7297 (1986).
8. R. Sullivan, J. A. Smith, M. Klagsbrun, *J. Cell. Biol.* **101**, 108a (1985); R. Lobb *et al.*, *J. Biol. Chem.* **261**, 1924 (1986); I. Vlodavsky *et al.*, *Proc. Natl. Acad. Sci. U.S.A.* **84**, 2292 (1987).
9. J. A. Abraham *et al.*, *Science* **233**, 545 (1986).
10. L. Schweigerer *et al.*, *Proc. Natl. Acad. Sci. U.S.A.* **84**, 842 (1987); N. Ferrara, L. Schweigerer, G. Neufeld, R. Mitchell, D. Gospodarowicz, *ibid.* p. 5773.
11. J. A. Abraham *et al.*, *EMBO J.* **5** (no. 10), 2533 (1986).
12. cDNA transcribed from poly(A)<sup>+</sup> mRNA of an AIDS-KS cell culture (AIDS-KS3) was cloned in the Eco RI site of  $\lambda$ gt10 phage and screened by hybridization with a mixture of the three oligonucleotide probes derived from the published cDNA sequences of human bFGF. The clones contained insert sizes of 0.45 to 1.4 kb. Three inserts of different sizes were subcloned into the Gemini vector system (pGEM 6-8: 0.67 kb; pGEM 24-15: 1.1 kb; pGEM 15: 1.25 kb) and sequenced (Gem-seq). The sequence analysis showed that the clones were of bFGF. The discrepancy in the transcripts when analyzed by RNA blotting from human and

## Dynamic Expression Pattern of the *myc* Protooncogene in Midgestation Mouse Embryos

PETER SCHMID, WOLFGANG A. SCHULZ,\* H. HAMEISTER

The *c-myc* protooncogene in mouse embryos was shown by RNA in situ hybridization to be preferentially expressed in tissues of endodermal and mesodermal origin. Most organs developing from the ectoderm, such as skin, brain, and spinal cord, displayed low levels of *c-myc* RNA. The thymus represented the only hematopoietic organ with high *c-myc* expression. In organs and structures strongly hybridizing to *c-myc* probes, for example the fetal part of the placenta, gut, liver, kidney, pancreas, submandibular glands, enamel organs of the molars, and skeletal cartilage, the level of expression depended on the stage of development. Expression was observed to be correlated with proliferation, particularly during expansion and folding of partially differentiated epithelial cells.

THE PRODUCT OF THE *c-myc* PROTOONCOGENE is thought to mediate the action of growth factors in many cell types (1). In general, *c-myc* expression seems to confer proliferation competence to cells and is switched off during terminal differentiation in differentiated leukemic cells of various lineages (2). To study the effect of *c-myc* on normal development and tumor formation, *c-myc* gene constructs have been introduced into the germ line of mice, allowing tissue-specific or generalized expression of its product (3). No gross developmental disturbances were observed in these transgenic animals, although tumor formation was increased in specific tissues or nonspecifically.

To study *c-myc* in normal development

Zimmerman *et al.* (4) observed *c-myc* expression in whole embryos beginning from day 15 of embryonic development, but specific tissues were not analyzed. In newborn mice, generalized expression of *c-myc* in different tissues was observed. In human embryos, Pfeifer-Ohlson *et al.* (5) investigated *c-myc* expression by RNA in situ hybridization with <sup>125</sup>I-labeled DNA probes. The *c-myc* expression was low in embryos at 3 to 4 weeks. However, embryos of 5 to 10 weeks displayed a high hybridization signal over

Abteilung Klinische Genetik der Universität Ulm, Oberer Eselsberg, D-7900 Ulm, Federal Republic of Germany.

\*Present address: Abteilung Biochemische Endokrinologie, Universitätskrankenhaus Eppendorf, Martinistrasse 52, 2000 Hamburg, Federal Republic of Germany.

epithelial cells of the skin and the intestine, as well as some connective tissues. Also, the cytotrophoblasts of the placenta became labeled.

We have determined the pattern of *c-myc* expression in mouse embryos by using single-stranded <sup>35</sup>S-labeled RNA probes (6), which appear to be more sensitive and specific in RNA in situ hybridization than DNA probes (7). Frozen sections of mouse embryos from days 12.5, 14.5, and 16.5 after coitus were probed with labeled RNA probes specific for exons 1, 2, or 3 of *c-myc*. Hybridization with sense-strand probes gave a uniformly distributed weak hybridization signal at all embryonal stages (Fig. 1B). This background signal was strongest with the sense probe for exon 1 (8), which could represent nonspecific binding of the probe or low amounts of *c-myc* antisense RNA (9).

Antisense probes for all three exons revealed an identical pattern of expression with slight differences in intensity. At all developmental stages examined, most of the embryo was labeled more strongly by antisense than by sense probes. At each stage, *c-myc* expression was much more pronounced in specific tissues (Fig. 1, A, C, and D, and Table 1). In contrast, the expression of  $\alpha$ -fetoprotein, studied as another control, was restricted to visceral endoderm and fetal liver and was stable throughout our period of observation (8).

In the 12.5-day embryo, *c-myc* expression as measured by a probe for exon 2 was most apparent in the fetal part of the placenta, specifically in the chorionic villi of the labyrinth (Fig. 2, A and B). Thus, expression occurs in the same cell type as in human placenta (5). Among individual villi, the signal was highly variable. Such heterogeneity could reflect differences in proliferation between individual cell clusters as reported in the human placenta (5). Specific hybridization to the maternal part of the placenta and the extraembryonic membranes that sustain erythropoiesis until around day 14 was not observed on day 12.5 or at any other stage.

The most intensely labeled organ of the fetus was the liver (Fig. 1A). Again the hybridization was discontinuously distributed. Hematopoietic foci, as revealed by hematoxylin and eosin staining, were mostly devoid of label (Table 1). The hepatocytes were heavily labeled, although the extent was variable. However, hepatocytes at this stage may not reflect a homogeneous population. Other organs of endodermal origin, such as the lung, pancreas, and other discernible parts of the embryonal gut, also had intermediate to high levels of *c-myc* expression (Fig. 1A). Although consisting of de-

termined cells, these organs are not yet functional at this stage. The metanephros anlage was also labeled; no discernible difference was observed between cortical and medullar regions. In contrast, the mesonephric tubules of the 10.5-day embryos did not exhibit conspicuous label (8). Because of their metameric arrangement, the precartilaginous masses of the cerebral vertebra, the spinal ganglia of the thoracic spinal cord, and somites 49 to 51 in the lumbar part appear prominent in Fig. 1A.

In the 14.5-day embryo expression was considerably reduced in the lung, liver, and placenta (8) (Fig. 1C). In the lung hybridization was confined to the bronchial mesenchyme. In the liver the signal was still restricted to hepatocytes. Megakaryocytes, which were identified easily by their large size, and other hematopoietic cells were only

weakly labeled. In contrast, all cells of the thymus were labeled strongly. At this stage, the thymus contains a heterogeneous, interspersed population of stromal cells and T cells at various stages of maturation. Aside from the thymus, the gut epithelium was the most prominent site of *c-myc* expression at day 14.5 (Fig. 2, C and D). No activity above background could be discerned in the mesodermal layers of the gut where lymphoblastoid organs were developing. In the kidney the hybridization signal appeared weaker than at day 12.5 and was confined to the tubular epithelia (8). Glomeruli were not labeled. Similarly, the epithelial layer of the branching tubules were the main sites of *c-myc* expression in the pancreas.

In the oral cavity the large tongue showed an unevenly distributed signal of intermediate intensity. The tooth buds of the first

**Fig. 1.** In situ hybridization analysis of *c-myc* expression in midgestation mouse embryos. The Xba I-Sac I fragment from SVmyc1 (18) containing mostly exon 2 was inserted into pBS (Genofit). Plasmids were linearized, and single-stranded <sup>35</sup>S-labeled RNA probes were prepared. All probes were subsequently reduced to 100 to 200 bases in length by partial hydrolysis. In situ hybridization was done with a modification of the procedure described (7). Deciduas and embryos were isolated from pregnant Rb (4.15) 4Rma mice and fixed immediately in 4% paraformaldehyde in phosphate-buffered saline. Cryostat sections of the embryos were placed on pretreated (7) 3-aminopropyltriethoxysilane-coated slides (19) and stored at -70°C. Prehybridization was at 54°C for 2 hours in 50% formamide, 10 mM tris, 10 mM sodium phosphate, pH 6.8, 20 mM dithiothreitol, 0.2% Denhardt's solution, 0.3M NaCl, *Escherichia coli* RNA (0.1 mg/ml), and 0.1 mM  $\alpha$ S-uridine triphosphate. Hybridization was carried out in the same solution supplemented with an RNA probe (80,000 cpm/ $\mu$ l) for 16 hours at 54°C. Slides were washed in hybridization solution for 2 hours and rinsed for 15 min in 0.5M NaCl, 10 mM tris, pH 7.5, and 1 mM EDTA. The remaining unhybridized RNA probe was digested with ribonuclease A. The slides were washed again, dehydrated, and air-dried. After initial x-ray autoradiography, they were coated with a 1:2 dilution of Ilford K5 emulsion and exposed for 3 weeks at 4°C. The slides were developed in Kodak D19 developer and stained with Giemsa or hematoxylin and eosin. Dark-field illumination of embryo sections after hybridization with antisense (A, C, and D) or sense (B) probe. (A and B) sagittal section of 12.5-day mouse embryo; (C) sagittal section of 14.5-day mouse embryo; (D) sagittal section of 16.5-day mouse embryo; k, kidney; li, liver; lu, lung; and t, thymus.

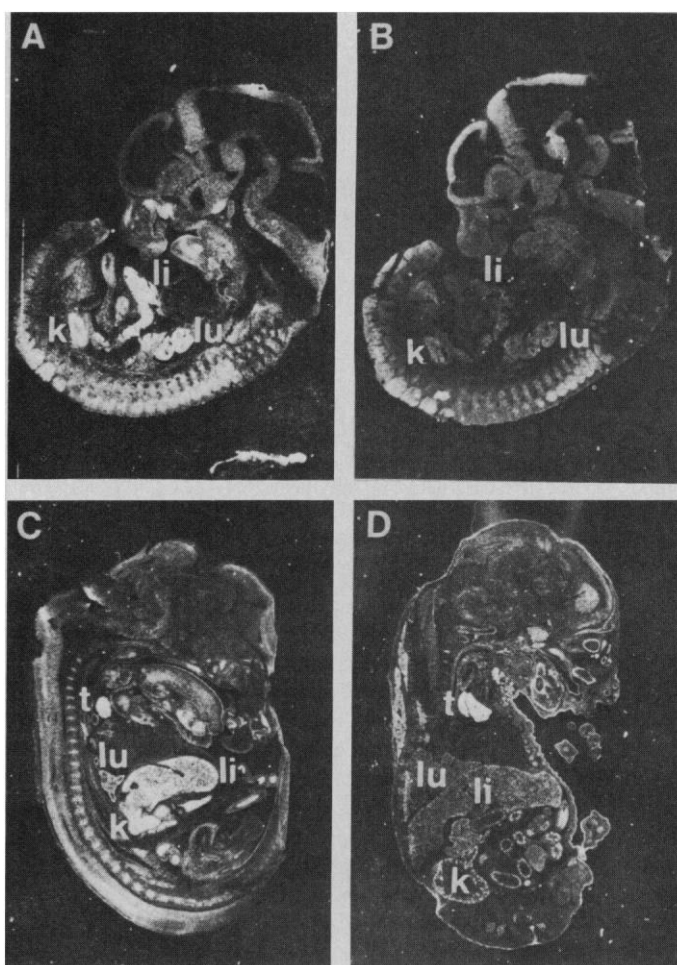


**Table 1.** Illustration of the dynamic mode of *c-myc* expression in selected organs of midgestation mouse embryos. Values were determined by counting silver grains over 100 individual cells for both sense and antisense RNA ( $\bar{x} \pm \text{SEM}$ ); >25 indicates an intense signal where individual grains are not discernible.

Tissue	<i>c-myc</i> expression					
	Day 12.5		Day 14.5		Day 16.5	
	Antisense	Sense	Antisense	Sense	Antisense	Sense
Fetal placenta	>25	4.6 ± 1.5	7.1 ± 2.3	4.2 ± 1.5		
Gut epithelium	9.7 ± 2.1	2.4 ± 1.1	>25	2.6 ± 1.3	17.4 ± 2.4	2.4 ± 1.3
Lung	>25	2.5 ± 1.3	18.8 ± 2.6	2.8 ± 1.3	8.5 ± 2.0	2.6 ± 1.5
Hepatocytes	>25	2.7 ± 1.5	17.2 ± 3.0	2.9 ± 1.5	6.6 ± 1.9	2.4 ± 1.2
Hematopoietic cells	5.5 ± 1.5	2.0 ± 1.2	4.5 ± 1.9	2.3 ± 1.2	6.4 ± 1.7	2.5 ± 1.2
Kidney	>25	3.2 ± 1.7	17.1 ± 2.5	2.1 ± 1.4	11.7 ± 2.0	2.2 ± 1.2
Thymus			>25	2.3 ± 1.2	>25	2.3 ± 1.2
Glandula submandibularis					>25	2.3 ± 1.2
Preadipocytes					19.5 ± 2.4	2.4 ± 1.3
Brain	5.4 ± 2.3	2.5 ± 1.3	7.1 ± 1.6	2.5 ± 1.3	3.5 ± 1.6	2.4 ± 1.2
Pancreas			>25	2.4 ± 1.3	12.8 ± 2.0	2.5 ± 1.3

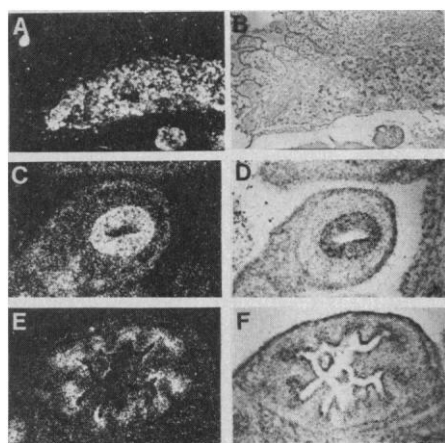


**Fig. 2.** Photographs of selected mouse embryo tissues after hybridization to a *c-myc* antisense probe. On the left dark-field and on the right bright-field illumination; (A and B) 10.5-day placenta, hybridization is restricted to the fetal part; (C and D) 14.5-day gut; (E and F) 16.5-day gut, hybridization confined to crypts.

molars in both the upper and lower jaws exhibited considerable *c-myc* expression in the enamel organ surrounding the dental papilla. At this stage the enamel epithelium is proliferating extensively while beginning cuspal morphogenesis (10). Thus, as in kidney, pancreas, gut, and liver, *c-myc* expression in molars coincided with the extension and folding of epithelial cell layers. As in other stages, the antisense probe hybridized only slightly more strongly to the brain and spinal cord than the sense probe. In contrast, the segmental pattern of the vertebra could be clearly discerned because of the specific labeling of the intervertebral disks.

In 16.5-day embryos, strong expression of *c-myc* was confined to the thymus and the glandula submandibularis (Fig. 1D). A lower level of expression was observed in the epithelia of the collecting tubules in the

kidney, the acini and ducts of the exocrine pancreas, and the intestine. Although at earlier stages the labeling of the gut epithelium had been uniform, a gradient of expression could now be discerned. The strongest labeling was found in the rapidly proliferating cells inside the crypts (Fig. 2, E and F). The change in *c-myc* expression thus seemed to follow the changing pattern of intestinal proliferation. In the liver and lung, the hybridization signal was even lower than at day 14.5 (Table 1). In the head the enamel organs of the first and second molar and the nasal-cavity epithelium displayed high *c-myc* expression. As observed in the 12.5- and 14.5-day-old embryos, several structures derived from the sclerotome hybridized specifically, notably the precartilag stages of the tracheal ring, the sternum, and the ribs. Dorsally the intervertebral disks were discernible. The strongest signal middorsally represents rapidly growing fat-cell precursors forming the brown fat tissue (11).

In conclusion, strong expression of *c-myc* was observed only in rapidly proliferating tissues, while *c-myc* was expressed to some extent in most, if not all, tissues of the mouse embryo; there was, however, preferential expression in tissues derived from the embryonal gut and certain parts of the mesoderm. Other structures derived from mesoderm, such as the heart, skeletal muscles, and mesodermal linings of skin and gut, did not display more than background levels of hybridization throughout our observation period. If a *c-myc*-like activity were indeed indispensable for cell proliferation, a different protein would have to substitute for *c-myc* in these tissues. Expression of *c-myc* seems to be restricted to a particular stage of cell differentiation in some organs. This would agree with the finding that *c-myc* may be expressed late in B cell development (12).

Its most significant role may be in the proliferation of determined, not yet completely differentiated cells during tissue expansion. Examples of these regions are the branching of renal tubuli, pancreatic and glandular epithelia, extension of hepatic trabeculae, and T cell development from lymphoid stem cells. This hypothesis might also explain the conspicuous lack of *c-myc* expression in the early lymphoid precursor cells in the yolk-sac mesoderm, liver, gut, and spleen.

Expression of *myc* is enhanced in many tissues of the embryo that are known to express *myc* after transformation in the adult. Elevated *c-myc* RNA has been found in T cell lymphomas (13), neoplastic (and hyperplastic) liver (14), some gastric adenocarcinomas (15), lung cancer (16), and polycystic kidney disease where epithelium-lined cysts are formed through extensive proliferation of renal tubules (17). Expression of *c-myc* in these rather well-differentiated tumors may represent a reversion to a fetal mode of proliferation.

#### REFERENCES AND NOTES

1. K. B. Marcu, *Bioessays* 6, 28 (1987).
2. K. Alitalo et al., *Biochim. Biophys. Acta* 907, 1 (1987); S. Cory, *Adv. Cancer Res.* 47, 189 (1986).
3. T. A. Stewart, P. K. Pattengale, P. Leder, *Cell* 38, 627 (1984); J. M. Adams et al., *Nature* 318, 533 (1985); A. Leder, P. K. Pattengale, A. Kuo, T. A. Stewart, P. Leder, *Cell* 45, 485 (1986).
4. K. A. Zimmerman et al., *Nature* 319, 780 (1986).
5. S. Pfeifer-Ohlson et al., *Proc. Natl. Acad. Sci. U.S.A.* 82, 5050 (1985); A. S. Goustin et al., *Cell* 41, 301 (1985).
6. D. A. Melton et al., *Nucleic Acid Res.* 12, 7035 (1984).
7. K. H. Cox, D. V. DeLeon, L. M. Angerer, R. C. Angerer, *Dev. Biol.* 101, 485 (1984).
8. P. Schmid, unpublished result.
9. M. S. Kindy, J. E. McCormack, A. J. Buckler, R. A. Levine, G. E. Sonenshein, *Mol. Cell. Biol.* 7, 2857 (1987).

10. A.-M. Partanen and I. Thesleff, *Differentiation* **34**, 25 (1987).
11. R. Rugh, *The Mouse* (Burgess, Minneapolis, MN, 1968).
12. W. Y. Langdon, A. W. Harris, S. Cory, J. M. Adams, *Cell* **47**, 11 (1986).
13. L. M. Corcoran, J. M. Adams, A. R. Dunn, S. Cory, *ibid.* **37**, 113 (1984).
14. R. C. Richmond, M. A. Pereira, J. H. Carter, R. E. Lang, *J. Histochem. Cytochem.* **36**, 179 (1988).
15. M. Shibuya, J. Yokota, Y. Ueyama, *Mol. Cell. Biol.* **5**, 414 (1985).
16. Y. Taya *et al.*, *EMBO J.* **3**, 2943 (1984).
17. B. D. Cowley, F. L. Smardo, J. J. Grantham, J. P. Calvet, *Proc. Natl. Acad. Sci. U.S.A.* **84**, 8394 (1987).
18. H. Land, F. Parada, R. A. Weinberg, *Nature* **304**, 596 (1983).
19. M. Rentrop, B. Knapp, H. Winter, J. Schweizer, *Histochem. J.* **18**, 271 (1986).
20. The overall photographs shown in Fig. 1 do occasionally mislead the observer. Besides artifactual signals, for example, on the edges, differences in tissue density may lead to false interpretations. True values for specific in situ hybridization are obtained only if grain densities over individual cells are determined and compared to the sense probe background (Table 1). Our description refers to such values and may therefore occasionally appear at odds with the overall photographs in Fig. 1.
21. Funded by a grant from the Deutsche Forschungsgemeinschaft to H.H. We wish to thank several colleagues for providing plasmid probes.

8 June 1988; accepted 19 October 1988

## Perineurium Originates from Fibroblasts: Demonstration in Vitro with a Retroviral Marker

MARY BARTLETT BUNGE, PATRICK M. WOOD, LAURA B. TYNAN, MARGARET L. BATES, JOSHUA R. SANES

**A cellular sheath, the perineurium, forms a protective barrier around fascicles of nerve fibers throughout the peripheral nervous system. In a study to determine the cellular origin of perineurium, a culture system was used in which perineurium forms after purified populations of sensory neurons, Schwann cells, and fibroblasts are recombined. Before recombination, the Schwann cells or the fibroblasts were labeled by infection with a defective recombinant retrovirus whose gene product,  $\beta$ -galactosidase, is histochemically detectable in the progeny of infected cells. Perineurial cells were labeled when fibroblasts had been infected but not when Schwann cells had been infected. Thus, perineurium arises from fibroblasts in vitro and, by implication, in vivo as well.**

**I**N VERTEBRATE PERIPHERAL NERVES, axons are ensheathed by Schwann cells (SCs), and fascicles of axon-SC units are encircled by perineurium. The perineurium consists of concentric, flattened cellular layers interspersed with clusters of collagen fibrils; individual perineurial cells are laden with vesicles and caveolae, extensively linked by tight junctions, and coated with basal lamina (basement membrane) on much of their surface (1, 2). The perineurium is virtually impermeable to all proteins that have been tested and restricts the passage of ions (for example, potassium and calcium) and small molecules (for example, glucose) (2). By forming a "tissue-nerve barrier," the perineurium regulates the endoneurial milieu and protects axons and SCs from antigens, toxins, infectious agents, and abrupt changes in ionic composition (2, 3). Perineurial protection against infection may be particularly important near body surfaces, where fascicles of sensory fibers frequently become exposed after injury. In addition, the perineurium may engender adjustments in nerve length by contractile mechanisms, as judged by the high incidence of actin filaments and associated subplasmalemmal dense bodies in perineurial cells (4).

A long-standing question about the perineurium is: What is its cellular source? Several candidates have been proposed (2, 5-7), but the two leading contenders have been SCs and fibroblasts (Fbs). (Occasional Fbs reside among axon-SC units, and Fbs form the cellular layers of the epineurium outside the perineurium.) When perineurium forms within developing (6) or regenerating (7) nerves in vivo, both Fbs and SCs are invariably present. In vitro, perineurium forms when pure populations of Fbs and SCs are combined with sensory neurons and cultured for several weeks; little or no perineurium forms when neurons are cultured with only Fbs or SCs (8, 9). However, it has been difficult to decide between Fbs and SCs as perineurial precursors because perineurial cells exhibit some properties of both cell types but are distinct from each one (10). Therefore, although indirect evidence favors the idea that perineurium arises from Fbs rather than SCs (7, 8), researchers studying peripheral nerve agree (1, 2, 5-7, 11, 12) that direct evidence on this point is lacking.

To resolve this issue, we have paired two recently developed techniques. The first is a method whereby separately cultured neurons, Fbs, and SCs can be recombined to

form a perineurium that exhibits many attributes present in vivo, that is, basal lamina, collagen fibrils, multiple cellular laminae, junctions of several types, and characteristic vesicles and caveolae (8, 9). The second is a method to permanently label the progeny of individual cells (13, 14). This method uses a recombinant retrovirus in which the *Escherichia coli lacZ* gene is substituted for retroviral structural genes. When the retrovirus infects a dividing cell, the *lacZ* gene integrates into the host genome and is inherited by daughter cells. The *lacZ*-encoded  $\beta$ -galactosidase, which we designate lacZ, catalyzes a histochemical reaction that yields a blue product visible by light microscopy and an electron-dense product detectable by electron microscopy. Most important for our purposes, the marker is not diluted by the numerous cell divisions that occur as the cultures develop. We were therefore able to prepare neuron-SC-Fb cultures containing either lacZ-positive Fbs or lacZ-positive SCs and then determine which combination gave rise to lacZ-positive perineurium.

Dorsal root ganglia from 15-day rat fetuses were dissociated, placed in culture, and treated with an antimetabolic agent to kill SCs and Fbs, leaving a purified neuronal population (15). The SCs cultured from separate ganglia were freed of Fbs as described (15), then resuspended and added to the neurons, whereupon they proliferated in response to a mitogen that axons present (16). Because the retrovirus infects only mitotically active cells (17), SCs were infected soon after addition to neurons to take advantage of the wave of SC proliferation that normally occurs; as expected, many axon-related SCs (~10% of the population) but no neurons became lacZ-positive. Embryonic Fbs were cultured from cranial periosteum and infected separately, then added to the neuron-SC cultures 3 weeks later when the neuritic outgrowth had become populated with SCs. After assembly of the neuron-SC-Fb cultures, the cells were given differentiation-supporting medium in which SCs myelinate axons (15). Recognizable perineurium formed by 6 weeks of culture, although full differentiation requires additional weeks (9). Retroviral infection did not retard development, as demonstrated by extensive myelination and perineurium formation in numerous cultures. After 6 to 8 weeks, the cultures were stained for lacZ (13) and prepared for microscopy (9, 18).

Our consistent result was that infected Fbs but not infected SCs gave rise to lacZ-positive perineurial cells. In whole mounts of cultures containing neurons, uninfected

Department of Anatomy and Neurobiology, Washington University School of Medicine, St. Louis, MO 63110.